The Effect of Buoyancy on Upward-Concurrent Flame Spread over Thin Paper

Maria Thomsen[1] and Carlos Fernandez-Pello[2]
Department of Mechanical Engineering, University of California, Berkeley, CA, 94720, USA

David L. Urban[3] and Gary A. Ruff[4]
NASA Glenn Research Center, Cleveland, OH, 44135, USA

Understanding material flammability inside a spacecraft is important because the conditions in spacecraft environments can greatly differ from those on earth. Because in a gravity field there is a flame-induced buoyancy, it is very difficult to reproduce on Earth the environmental conditions of a spacecraft, thus making fire testing harder. To overcome this problem, alternative approaches that reduce buoyancy are required. One possibility to reduce buoyancy effects relies in using reduced ambient pressure. The objective of this work is to study the effect of pressure, and consequently buoyancy, on upward/concurrent flame spread over a thin combustible solid, and by comparison with partial gravity data, observe up to what point low-pressure can be used to replicate flame characteristics observed in different gravity levels. Experiments in normal gravity were conducted over pressures ranging between 100 and 30 kPa and a forced flow velocity of 10 cm/s. Results show that reductions of pressure slow down the flame spread over the material surface. As pressure is reduced, flame intensity is also reduced. Comparison with partial gravity data shows that as the pressure is reduced, the normal gravity flame spread rate approaches that observed at different gravity levels. The data presented is correlated in terms of a mixed convection non-dimensional number that describes the convective heat transferred from the flame to the solid, and that also describes the primary mechanism controlling the spread of the flame. The correlation provides information about the similitudes of the flame spread process in variable pressure, flow velocity and gravity environments, providing guidance for potential ground-based testing for fire safety design in spacecraft.

I. Introduction

FIRE safety inside a spacecraft is an important concern when thinking about space travel, particularly when planning longer missions such as human missions to Mars. Cabin environments used during those missions may vary from normal atmospheres currently used on board the International Space Station (ISS). They may include very low velocity flows induced by the ventilation system, reduced cabin pressure (~60 kPa), increased oxygen concentration (~34% by vol.), and partial or microgravity[1,2]. Because a fire in a spacecraft could have catastrophic consequences, it is critical to understand how these environmental variables affect the parameters normally used to assess the flammability of a particular material.

Flame spread is one of the metrics commonly used to determine the material flammability of solid fuels. For example, NASA relies on an upward flame spread test to screen materials to be used in spacecraft cabins[3]. An upward/concurrent configuration is assumed in this test since as the flame spreads over the solid it covers the virgin fuel ahead of the pyrolysis front, which makes the heating and pyrolysis of the material faster and more hazardous than opposed (downward) flame spread. The spread of fires has been widely studied in the past[4–10], and over the years,

[1] Postdoctoral Researcher, Department of Mechanical Engineering, 60 Hesse Hall, University of California, Berkeley, CA, 94720, USA.
[2] Professor, Department of Mechanical Engineering, 6105A Etcheverry Hall, University of California, Berkeley, CA, 94720, USA.
[3] Physical Scientist, Space Technology Office, 21000 Brookpark Road, MS 77-7, Cleveland, OH, 44135, USA.
[4] Chief, Combust. and Reacting Systems Branch, 21000 Brookpark Road, MS 77-5, Cleveland, OH, 44135, USA.

researchers have investigated the differences between flame spread in normal gravity (1g) and microgravity (μg) by considering different parameters such as geometry[11–13], low flow velocities[14–16], oxygen concentration[11,14,15,17], or radiant heat flux[17]. Given the complex characteristics of upward flame spread, i.e. flames tend to be bigger and more uncontrolled[13], there are fewer experiments that focused on concurrent flow flame spread in microgravity environments.

The challenges associated with microgravity experiments (cost, duration, safety regulations, among others) make testing in space or other microgravity facilities difficult, so researchers have to look at alternative methods. A possible approach is to reduce the ambient pressure, and consequently density, to diminish the effect of gravity. In the particular case of concurrent flame spread, the ambient pressure affects the thickness of the boundary layer, and consequently the position of the flame with respect to the solid surface[7]. As the pressure is reduced the boundary layer thickens, the flame moves away from the surface, and the heat transferred from the flame to the solid surface is reduced. Consequently, the flame spread rate decreases because of the reduced heat flux on the surface and a reduction in the flame length[18]. Thus, the effect on the flame characteristics and the spread rate, of reducing the ambient pressure is like that of reducing the flow velocity. This is relevant because the primary obstacle to simulating flame spread in spacecraft environments in normal gravity is that the low flow velocities encountered in spacecraft (~0.1 m/s) cannot be attained in normal gravity because the buoyant flow (~0.4 m/s) overwhelms the forced flow. Following this analysis, several studies have taken advantage of the changes in buoyancy resulting from reducing pressure to simulate conditions encountered in microgravity[19–23].

Understanding the effect of gravity and other environmental conditions on solid material burning is important for improving strategies for NASA spacecraft materials selection. The goal of this work is to better understand upward/concurrent flame spread in micro or partial gravity environments over thin solids. Furthermore, the work presented here aims to link the burning behavior encountered at those reduced gravity conditions with experimental results obtained at reduced ambient pressure environments, investigating the similitudes between the two.

II. Experiments

The normal gravity experiments were conducted in an apparatus previously developed to study the flammability of solid combustible materials under varied ambient conditions[22,23]. The apparatus consists of a laboratory scale combustion tunnel that is inserted in a pressure chamber (Fig. 1). The tunnel has a 125 mm square cross section and a 600 mm total length. The first 350 mm section of the duct serves as a flow straightener, the other 250 mm segment of the duct is used as the test section. The chamber is provided with a flow system that provides constant supply and exhaust of gases to avoid vitiation problems. Compressed house air was supplied through critical nozzles (O'Keefe Controls) to the bottom of the duct while constantly evacuating to maintain constant pressure inside the chamber. The chamber pressure was controlled by a high-capacity vacuum generator (Vaccon JS-300) and a mechanical vacuum regulator. The chamber pressure was monitored constantly with an electronic pressure transducer (Omega Engineering, Inc. PX303-015A5V). The tests were conducted in air under pressures ranging between 30 and 100 ± 2 kPa. The forced flow was adjusted to provide 10 cm/s at the respective chamber pressure for all tests, this velocity was selected to match the flow of air induced by the HVAC system inside of a spacecraft. In addition to the forced flow, because the experiments were performed under normal Earth's gravity, the flame is also exposed to a buoyant flow induced by itself that changes as a function of ambient pressure. Thus, during the experiments the flame is exposed to a mixed flow condition with a flow velocity that changes with pressure. The direction of the flow and the flame spread were upward, so the flame was in the concurrent configuration.

The samples presented in this work were selected to match previous experiments at different gravity levels and ambient pressure conducted by Kleinhenz et al.[20]. The thin solid is a cellulosic tissue with the trade name of "Kimwipes, Delicate Task Wipers" manufactured by the Kimberly-Clark Corporation. The area density of the material is 2.08 ± 0.16 mg/cm^2. The samples tested were cut into rectangular pieces and were held in between two identical stainless-steel frames 0.6 mm thickness, with a rectangular opening of 150 mm long by 50 mm wide (see right side picture of Fig. 2) that served as the test area. Each sample was placed vertically at the midplane of the test section. Ignition of the material is induced with a 29-gage Kanthal 45 mm length wire braided along the upstream edge of the sample. The igniter is energized using a controlled current power supply (BK Precision 1785) set to deliver 40 W for 2 s.

Two 9000 lumen LEDs were installed to help visualize and measure flame spread rate. The LEDs were turned on during the tests when the propagation of the pyrolysis front was measured and kept off for tests when visible flame size and shape was observed. The ignition and subsequent flame spread were video recorded with a resolution of 1280 by 720 at 59 frames per second using a Nikon D3200 camera to track the pyrolysis front. A second camera (Sony

RX10-III) was used to record videos of visible flame length with a resolution of 1280 by 720 at 59 frames per second. For each test condition, at least five replicate experiments were conducted to address the experimental uncertainty.

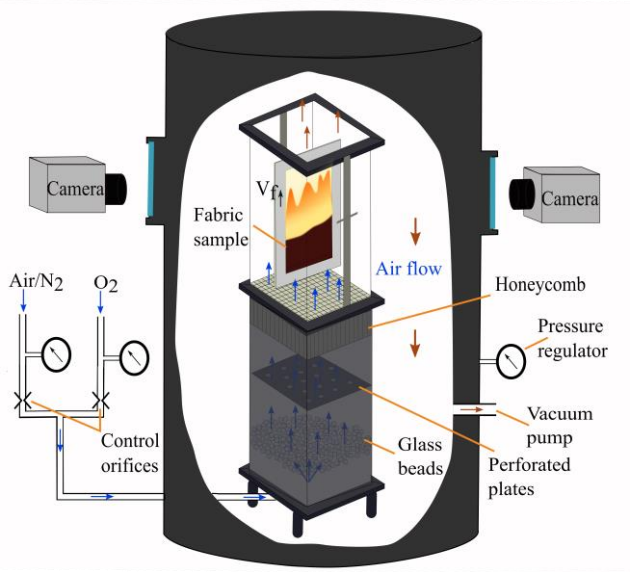

Figure 1. Schematic of experimental apparatus.

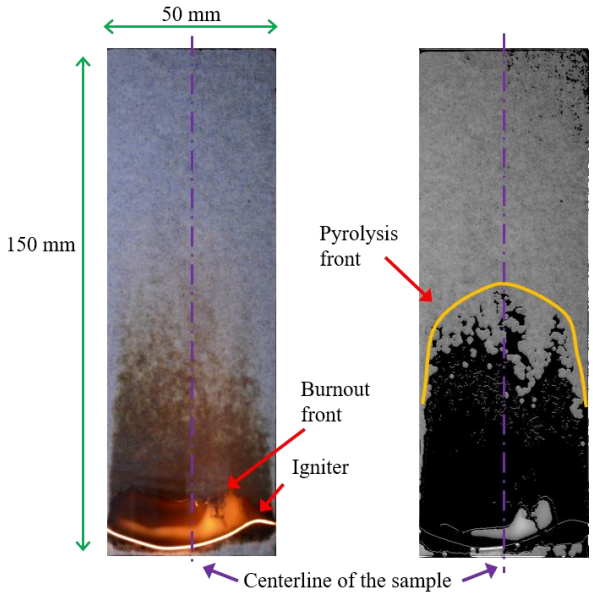

Figure 2. Photograph of a thin sample used for the experiments (left) and photograph used for the post-processing and determination of the pyrolysis front position (right).

III. Results

From video recordings the flame spread rate is measured as the evolution of the pyrolysis front position along the surface of the material over time. For these thin samples the pyrolysis front position is defined as the point on the sample where it first gets visibly blackened. Videos recorded during the experiments are corrected for perspective issues, then a threshold value is applied together with morphological corrections (opening and closing) to remove part of the noise and help in the determination of the pyrolysis front position, as shown in right side photograph of Fig. 2.

During each test, after ignition is achieved, the flame spreads uniformly along the surface of the sample. The pyrolysis front had an inverted "U" shape in all tests. As the flame spreads over the material surface it consumes almost all the tissue. Sometimes at the lower pressure conditions, some ash residue was left behind near the edges of the holder after the flame burned out. Figure 3 shows still photographs of the visible flame as it spreads over the solid at different ambient conditions, all photographs were taken with the same camera settings to show the effect of the environment on the visible flame. It is seen that as pressure is reduced the flame brightness is also reduced. As the material burns, significant soot is produced resulting in a very bright yellow/orange flame that becomes dimmer at the lower pressure environments. Fig. 3 also shows the burnout front as the flame begins receding over the surface, consuming the solid fuel.

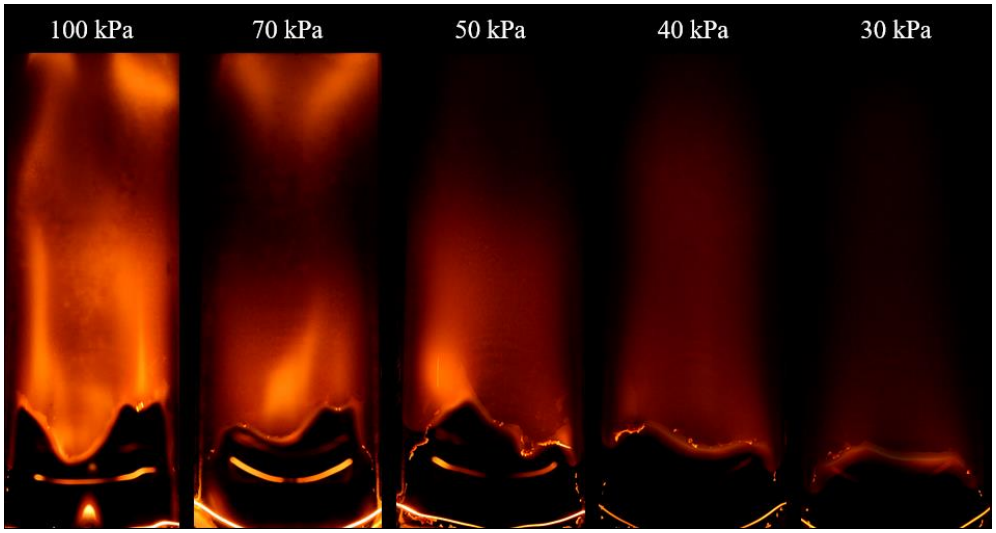

Figure 3. Effect of ambient pressure on flame appearance.

Figure 4 shows a characteristic result of the time evolution of the pyrolysis front for ambient pressures ranging between 100 and 30 kPa. It is seen that as pressure is reduced the spread of the flame is slower. The time dependence of the pyrolysis front is fairly linear for all pressures tested indicating an approximately constant flame spread rate, probably due to the high flammability of the material.

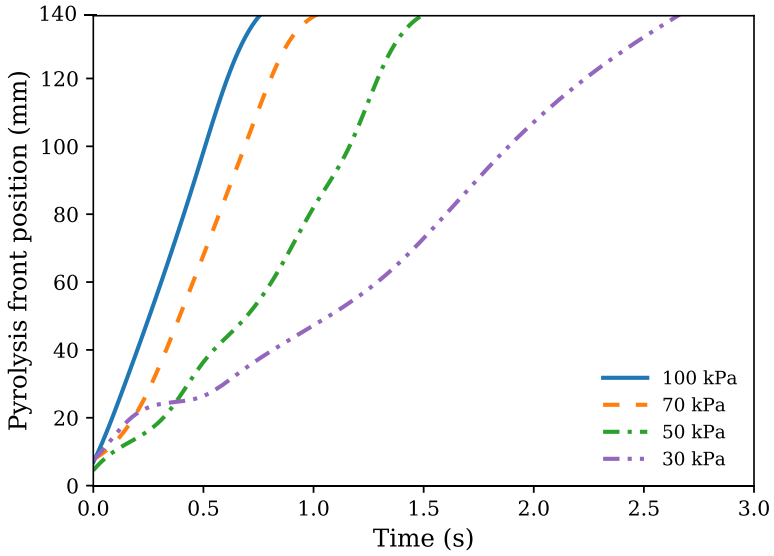

Figure 4. Time evolution of the pyrolysis front position of a representative test for different ambient pressures.

From each of the experimental conditions, an average flame spread is obtained from the progress of the pyrolysis front along the centerline of the sample. Figure 5 shows the average flame spread rate as a function of ambient pressure as obtained from the pyrolysis front data of Fig. 4. For comparison purposes, the flame spread rate data obtained by Kleinhenz et al.[20] at different ambient pressures and gravity levels is also included in the figure. From the figure it is seen that the flame spread rate is proportional to both the ambient pressure and the gravity level. For the present work, the normal gravity flame spread rate decreases from an average of 200 to 71 mm/s as the ambient pressure is decreased from 100 to 30 kPa. Using the partial gravity data of Kleinhenz et al.[20], together with the data of this work, it is seen that for a constant pressure of about 40 kPa the flame spread rate decreases from 92 mm/s to 39 mm/s and then to 19 mm/s when changing gravity from Earth gravity to Martian gravity and then to Lunar gravity. It is also seen that further reductions in ambient pressure and normal gravity will result in flame spread rates that are comparable in magnitude to those observed at Martian or Lunar gravities and different ambient pressures conditions. These results are an indication that concurrent flame spread in low pressure and normal gravity, may have similar characteristics as that in reduced gravity. It should be kept in mind however, that the total pressure reduction necessary to see these similarities will vary depending of the material and environmental conditions used [22–24].

It is important to mention that the differences that arise between the normal gravity flame spreads measured as part of this work and the results reported by Kleinhenz et al.[20], particularly at 30 kPa, are most likely due to the different flow conditions used. In the present work for all tests, an upward forced flow of 10 cm/s was applied to supplement the natural convective buoyant flow, whereas the experiments in Ref. [20] were performed with no forced flow.

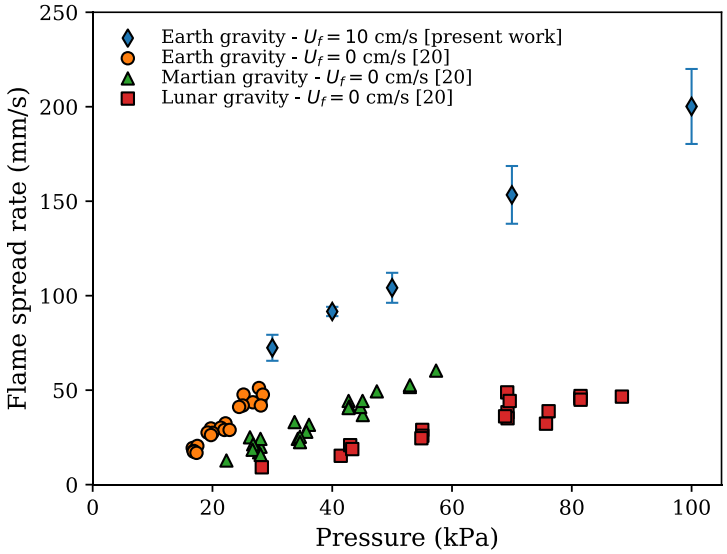

Figure 5. Flame spread rate as a function of ambient pressure.

An important parameter for concurrent flame spread is the pyrolysis length since it is directly proportional to the flame length and consequently the heat transferred from the flame to the solid. The variation of the pyrolysis length with pressure is presented in Fig. 6. The pyrolysis length is obtained as the difference between the pyrolysis front position and the burnout front position toward the end of the test. Given the unstable characteristic of the burnout front, and to be consistent with the measurements of the pyrolysis front position, the pyrolysis length is also measured along the centerline of the sample. It is seen that in normal gravity the pyrolysis length decreases with decreasing ambient pressure. However, the change is not as pronounced as with the flame spread rate. The reason for this could be related to the size of the sample not being long enough, the non-uniformity of the burnout front profile, and the fact that the material cracks and wrinkles as it starts burning.

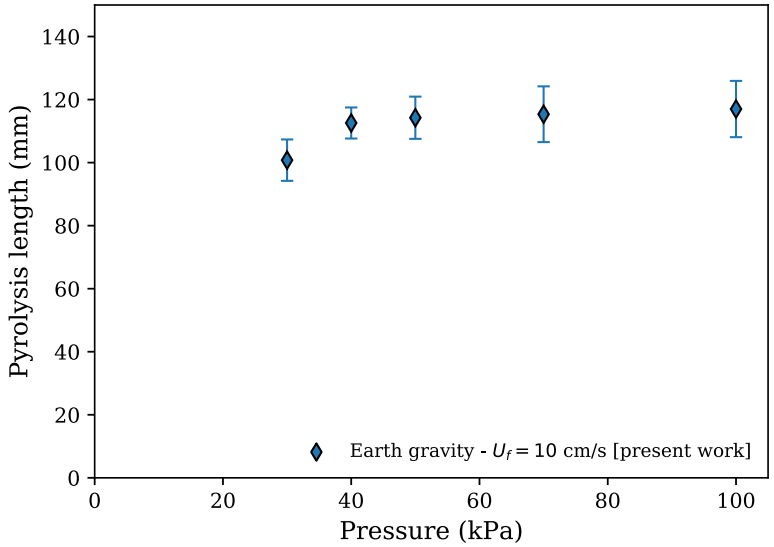

Figure 6. Pyrolysis length as a function of ambient pressure.

Reduced ambient pressure in 1-g has been used in previous studies because it can produce similar burning behaviors to those observed in microgravity conditions[19,22,23]. Kleinhenz et al.[20] considered the use of pressure-gravity modeling to simulate upward flame spread and burning rates in different gravity environments. As part of their results, the authors proposed that the data could be correlated by the expression $P^{1.8}g$ where P is the ambient pressure and g is the gravity level. Following a similar approach, the data of Fig. 5 was correlated in terms of pressure and gravity and the results are presented in Fig. 7. It is seen that the present data are correlated well with the same pressure and oxygen concentration relation and that the correlation works fairly well, however the data seems to diverge a bit for the higher pressures and gravity considered.

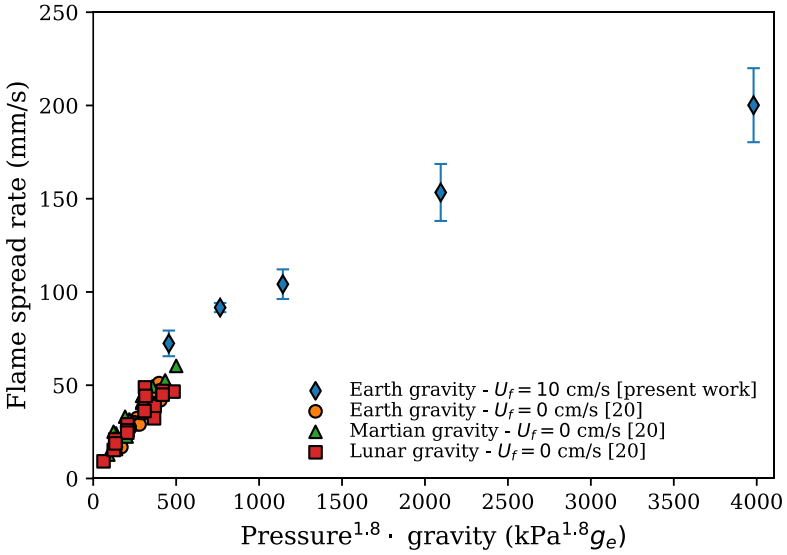

Figure 7. Flame spread rate as a function of the relation of pressure and gravity determined by Kleinhenz et al[20].

IV. Simplified Analysis and Discussion

Flame spread over a thin solid fuel can be analyzed in terms of the interactions between the different mechanisms involved in the spread process. To better understand the dependence of the flame spread rate on pressure and its

relation with partial gravity conditions, it is helpful to use a simplified analysis such as that developed by Fernandez-Pello[7]. The analysis provides an analytical equation for the concurrent flame spread rate as:

$$V_f = l_h \left[\frac{\rho_s c_s s (T_p - T_o)}{\dot{q}''_{fc} + \dot{q}''_{fr} - \dot{q}''_{rs}} - \frac{C_1 x}{U} t_{chem} \right]^{-1} \quad (1)$$

Where l_h is the heated length, $\dot{q}''_{fc}$ represents the convective heat flux at the solid surface, $\dot{q}''_{fr}$ is the flame radiant flux, $\dot{q}''_{rs}$ the re-radiation from the solid, U is the flow velocity, t_{chem} is a non-dimensional chemical time, ρ_s and c_s are the solid density and specific heat and s is the solid thickness. T_p and T_o represent the pyrolysis and initial temperatures of the solid. The first term in Eq. (1) describes the heat transfer mechanisms of the flame spread process and the second term represents the finite-rate, gas phase chemical kinetic effects. The contribution of the chemical term is small until the pressure becomes of the order of 30 kPa[25] or lower. Given the approximate nature of this analysis, it is assumed that the radiant flux from the flame to the solid approximately balances the surface re-radiation. This is a significant simplification that allows to develop a correlation for the flame spread rate with convective heat transfer as the dominant mechanism, and that can be sustained given the small size of the samples used for the tests. In Ref. [26] it was shown that as the sample size increases, and the flames becomes more turbulent the radiant flux becomes more important eventually dominating the heat transfer from the flame to the solid. The size of the sample would also affect the characteristics of the flame and the convective heat flux from flame to solid. It is important to mention that this assumption breaks down at very low velocity, low pressure or microgravity, flows where the flame stand-off distance may be large enough that re-radiation from the surface becomes larger than both convective and radiation heat transfer from the flame to the solid.

Then, the flame spread rate is primarily determined by the product of the flame heated length, l_h, and the convective heat flux, $\dot{q}''_{fc} = h\left(T_f - T_p\right)$, with h representing the convective heat transfer coefficient and T_f is the flame temperature. Based on a thermodynamic analysis, adiabatic flame temperature is proportional to the oxygen concentration and is not dependent on ambient pressure if the gases behave following the ideal gas law. Kinetically, the flame temperature is not strongly dependent on ambient pressure until the pressure gets low enough and the chemical time starts to become larger than the physical time. Thus, it is considered constant in the range of the present experiments. The heating length is related to the pyrolysis length[27] as $l_h \sim C l_p$. Under these conditions the flame spread rate becomes

$$V_f \sim l_p \left[\frac{h(T_f - T_p)}{\rho_s c_s s (T_p - T_o)} \right] \quad (2)$$

From Eq. (2) it is seen that the flame spread rate is proportional to the convective heat transfer coefficient at the solid surface, which in turn depends on ambient pressure. For a mixed flow, free and forced, such as that of the present experiments, the average convective heat transfer coefficient can be expressed in terms of the Reynolds Number and the Grashof number as[28].

$$h = C_2 \frac{k}{l_p} (Re^4 + Gr^2)^{1/8} Pr^{1/3} \quad (3)$$

Where $Re = \rho U_f l_p / \mu$ and $Gr = g\beta \Delta T l_p^3 \rho^2 / \mu^2$. Here l_p is the pyrolysis length which is taken as the solid surface characteristic length in the flow direction, U_f is the forced gas velocity, μ is the dynamic viscosity, ρ is gas phase density, β is the coefficient of thermal expansion and g is gravity level. It is seen that the heat flux at the surface is determined by a mix flow non-dimensional parameter that is a combination of the Grashof and Reynolds numbers. Furthermore, the heat transfer coefficient obtained from Eq. (3) is directly related to the boundary layer thickness through $h = k/\delta$, and the boundary layer thickness is directly related to the gas flow velocity. Thus, the data presented in Fig. 5 could be correlated in terms of an equivalent gas flow velocity so that when applied in a forced flow analysis will produce a boundary layer similar to that of the mixed flow. This equivalent flow velocity could then be incorporated in the concurrent forced flame spread rate equation (Eq. (2)) to predict the flame spread rate in a mixed flow.

Following this approach, the equivalent gas flow velocity can be obtained by equating the boundary layer thickness for a forced flow, given by

$$\delta_f = l_p Re^{-1/2} Pr^{1/3} \tag{4}$$

With that for a mixed convective flow, given by

$$\delta_m = l_p (Re^4 + Gr^2)^{-1/8} Pr^{1/3} \tag{5}$$

It is seen that, as the ambient pressure changes, the thicknesses of both boundary layers vary as $\delta \propto P^{-1/2}$. Thus, the boundary layer gets thicker for lower values of the flow velocity and pressure, which results in a less elongated shape of the flame and a lower convective heat flux on the solid surface. Equating the boundary layer thicknesses for a pure forced flow (Eq. (4)) and a mixed convection flow (Eq. (5)), the following equivalent velocity, U_{eq}, is obtained in terms of pressure, forced flow velocity, and gravity. This equivalent velocity is a gas flow velocity, corrected by pressure, that could be applied in a force flow condition in microgravity or partial gravity.

$$U_{eq} = \frac{P}{P_0} U_f \left(1 + \frac{g^2 l_p^2}{U_f^4}\right)^{1/4} \tag{6}$$

where P_o is a reference ambient pressure (standard Earth ambient pressure) and U_f is the forced flow at this reference pressure $P_o = 100\ kPa$. From Eq. (6) it is seen that for low gravity or large flow velocity the equivalent velocity is that of a purely-forced flow at a given test pressure, $U_{eq} = \frac{P}{P_0} U_f$. For elevated gravity and/or low forced velocity, the equivalent gas flow velocity becomes that of natural convection at a given test pressure, $U_{eq} = \frac{P}{P_0} (g l_p)^{1/2}$. This later expression is also somewhat consistent with the results of Kleinhenz et al.[20] for a purely-buoyant flow and their correlation of $P^{1.8} g$.

At a given forced flow velocity and gravity level as the pressure is reduced the equivalent velocity is also reduced. The velocity of Eq. (6) would produce an equivalent forced flow boundary layer of similar thickness as that of the mixed convective flow, and consequently an approximately similar convective heat flux on the fuel surface. Considering also that the gas phase density can be scaled with pressure, the resulting convective heat transfer coefficient is

$$h \sim C_3 \frac{k}{l_p} \left(\frac{U_{eq} P l_p}{\mu}\right)^{1/2} Pr^{1/3} \tag{7}$$

and the flame spread would be given by

$$V_f = C_3 l_p \left[\frac{\frac{k}{l_p} \left(\frac{U_{eq} P l_p}{\mu}\right)^{1/2} Pr^{1/3} (T_f - T_p)}{\rho_s c_s s (T_p - T_o)}\right] \tag{8}$$

Eq. (6) can be used to plot the normal gravity, low pressure data with the partial gravity, low pressure data in common coordinates. Figure 8 shows the flame spread data of Fig. 5, but this time presented as a function of the equivalent gas flow velocity obtained from Eq. (6). From the figure it can be noted that as pressure is reduced the equivalent flow velocity also changes, becoming closer to what is observed during the different partial gravity tests. Also worth noting is that when the data is presented in terms of the equivalent gas flow velocity, it seems to align fairly well with the partial gravity data obtain at all conditions.

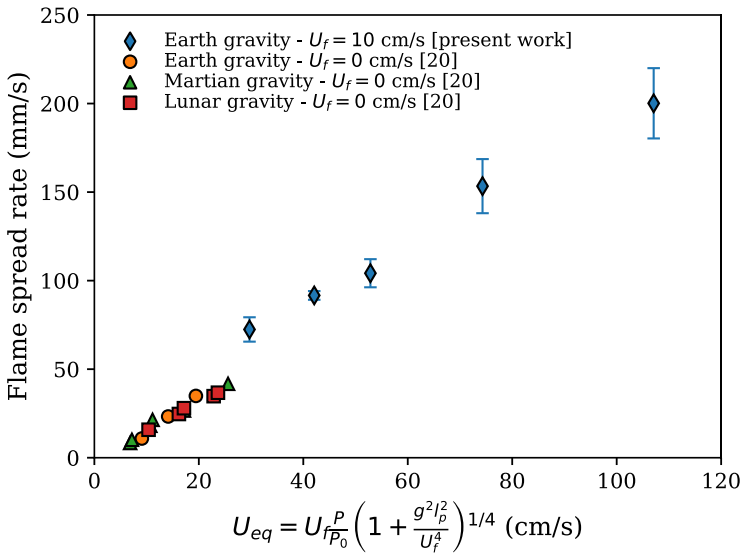

Figure 8. Flame spread rate as a function of the mixed flow velocity.

Another similar alternative approach can also be used to correlate the data at different gravity levels, using the data obtained at reduced pressure environments so that the gas flow velocity remains the same as that at reduced gravity. Thus, the reduced pressure test results presented in Fig. 5 could be correlated in terms of the gravity level. This theoretical gravity level, obtained from the reduced pressure tests, would produce a boundary layer of the same thickness as that encountered if the equivalent gas flow velocity were to be applied in a purely forced flow as in a microgravity environment and normal ambient pressure. Starting with the equivalent velocity of Eq. (6) and equating that to the velocity that would be applied to a purely forced flow condition, the equivalent partial gravity, g, can be determined as follows

$$g_{(P=P_0)} = \frac{1}{l_p}\left(\left(\frac{U_{eq} P_0}{P}\right)^4 + U_f^4\right)^{1/2} \tag{9}$$

Figure 9 presents the results of Fig. 5 as a function of the gravity level obtained from Eq. (9). From the figure it is seen that Eq. (9) works well in correlating the data obtained at lower pressure and different gravity environments. As ambient pressure is reduced, the resulting equivalent flow velocity is also reduced (as shown in Fig. (8)) independent of the gravity level considered, and thus the equivalent gravity level is also reduced, resulting in lower flame spread rates.

It is worth noting that a similar results were also obtained when correlating the concurrent flame spread rate dependence on pressure for other thermally thin[22,24] and thick[23] solid fuels.

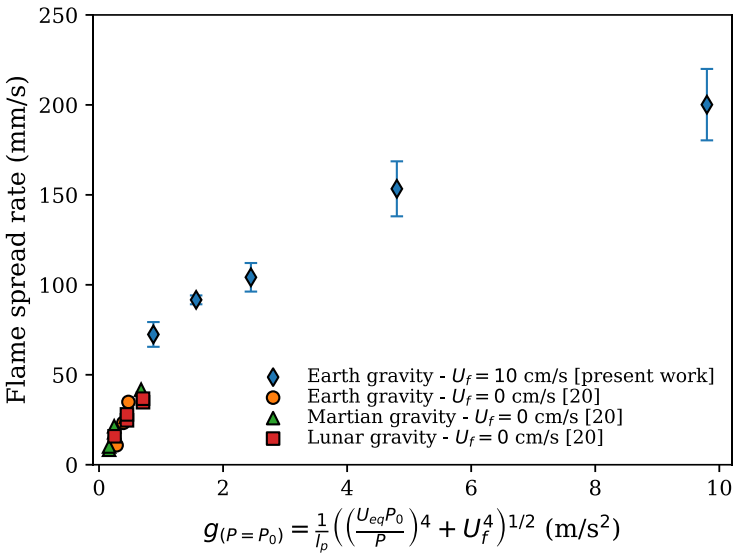

Figure 9. Flame spread rate as a function of gravity level.

The results of Fig. 8 and 9 show that the concurrent flame spread in different gravity conditions, such as on Mars or the Moon, can be simulated by reducing the ambient pressure to levels of the order of 20 kPa. It is important to keep in mind that that absolute pressure reduction required to replicate micro or partial gravity data is going to be dependent on the material and the conditions that are to be replicated. Also, care should be taken at very low-pressure levels where chemical kinetic effects can start to become important and affect the flame spread process, making the predictions given by the analysis less accurate.

V. Conclusion

The concurrent flame spread rate and flame appearance of a burning thin cellulosic solid has been studied under different reduced ambient pressure conditions to determine if it is possible to simulate the primary flame properties obtained in partial gravity environments by reducing the ambient pressure. It has been found that as pressure is reduced, the flame spread rate over the solid material is also reduced. Flame intensity is also weakened resulting in dimmer flames. A reduction in ambient pressure to around 20 kPa results in flame spread rates values that approached the spread rate observed in gravity levels such as those of Mars or the Moon. The correlation of the flame spread rate data in terms of mixed flow parameters that includes gravity and pressure suggests that reduced pressure can be used to simulate untested levels of gravity conditions.

It should be kept in mind that variations in ambient pressure can affect flame chemistry, particularly at the very low ambient pressures (below 20 kPa). At those very low pressures, the gas phase chemical reactions become slower, affecting the heat provided by the flame to the unburned solid and therefore reducing the flame spread rate. Thus, care should be taken with how these results are interpreted and used to predict flame spread at different gravity levels, particularly because eventually low pressure will affect the chemical kinetics of the process.

Acknowledgments

This research was supported by NASA Grant NNX12AN67A. The authors would like to thank Tony Wu, Alina Rai, Kevin Chung, Christina Liveretou, Aram Cariaga, Nathan Ngoy, Hemant Chaudhary, Sonja Davison, Jung Ahn, and Jiaxuan Yang for their help conducting the experiments.

References

1. Friedman, R. Fire Safety in Spacecraft. *Fire Mater.* **20**, 235–243 (1996).
2. Lange, K. E., Perka, A. T., Duffield, B. E. & Jeng, F. F. *Bounding the Spacecraft Atmosphere Design Space for Future Exploration Missions*. (2005).
3. National Aeronautics and Space Administration. *NASA-STD-6001B Flammability, Offgassing, and Compatibility Requirements and Test Procedures*. (2011).

4. Bhattacharjee, S., Altenkirch, R. A., Srikantaiah, N. & Vedhanayagam, M. A Theoretical Description of Flame Spreading over Solid Combustibles in a Quiescent Environment at Zero Gravity. *Combust. Sci. Technol.* **69**, 1–15 (1990).
5. Fernandez-Pello, A. C. & Hirano, T. Controlling mechanisms of flame spread. *Combust. Sci. Technol.* **32**, 1–31 (1983).
6. Markstein, G. H. & De Ris, J. Upward fire spread over textiles. *Symp. Combust.* **14**, 1085–1097 (1973).
7. Fernandez-pello, C. The solid phase. in *Combustion Fundamentals of Fire* (ed. Cox, G.) 31–100 (Academic Press Limited, 1994).
8. Quintiere, J. A simplified theory for generalizing results from a radiant panel rate of flame spread apparatus. *Fire Mater.* **5**, 52–60 (1981).
9. Wichman, I. S. Theory of opposed-flow flame spread. *Prog. Energy Combust. Sci.* **18**, 553–593 (1992).
10. Olson, S. L., Ruff, G. A. & Miller, F. J. Microgravity Flame Spread in Exploration Atmospheres: Pressure, Oxygen, and Velocity Effects on Opposed and Concurrent Flame Spread. in *38th International Conference on Environmental Systems* 1–8 (2008). doi:10.4271/2008-01-2055
11. Kikuchi, M., Fujita, O., Ito, K., Sato, A. & Sakuraya, T. Experimental study on flame spread over wire insulation in microgravity. *Symp. Combust.* **27**, 2507–2514 (1998).
12. Link, S., Huang, X., Fernandez-Pello, C., Olson, S. & Ferkul, P. The Effect of Gravity on Flame Spread over PMMA Cylinders. *Sci. Rep.* **8**, 120 (2018).
13. Urban, D. L., Ferkul, P., Olson, S., Ruff, G. A., T'ien, J. S., Liao, Y. T., Fernandez-pello, A. C., Torero, J. L., Legros, G., Eigenbrod, C., Smirnov, N., Fujita, O., Rouvreau, S., Toth, B., Jomaas, G. Flame Spread : Effects of Microgravity and Scale. *Combust. Flame* **199**, 168–182 (2019).
14. Olson, S. L., Ferkul, P. V. & T'ien, J. S. Near-limit flame spread over a thin solid fuel in microgravity. *Symp. Combust.* **22**, 1213–1222 (1988).
15. Olson, S. L. Mechanisms of Microgravity Flame Spread Over a Thin Solid Fuel: Oxygen and Opposed Flow Effects. *Combust. Sci. Technol.* **76**, 233–249 (1991).
16. Grayson, G., Sacksteder, K. R., Ferkul, P. V. & T'ien, J. S. Flame spreading over a thin solid in low-speed concurrent flow- Drop tower experimental results and comparison with theory. *Microgravity Sci. Technol.* **VII**, 187–195 (1994).
17. Osorio, A. F., Mizutani, K., Fernandez-Pello, C. & Fujita, O. Microgravity flammability limits of ETFE insulated wires exposed to external radiation. *Proc. Combust. Inst.* **35**, 2683–2689 (2015).
18. Ferkul, P. V. & T'ien, J. S. A model of low-speed concurrent flow flame spread over a thin fuel. *Combust. Sci. Technol.* **99**, 345–370 (1994).
19. Nakamura, Y., Yoshimura, N., Ito, H., Azumaya, K. & Fujita, O. Flame spread over electric wire in sub-atmospheric pressure. *Proc. Combust. Inst.* **32**, 2559–2566 (2009).
20. Kleinhenz, J., Feier, I. I., Hsu, S. Y., T'ien, J. S., Ferkul, P. V., Sacksteder, K. R. Pressure modeling of upward flame spread and burning rates over solids in partial gravity. *Combust. Flame* **154**, 637–643 (2008).
21. Fereres, S., Fernandez-Pello, C., Urban, D. L. & Ruff, G. A. Identifying the roles of reduced gravity and pressure on the piloted ignition of solid combustibles. *Combust. Flame* **162**, 1136–1143 (2015).
22. Thomsen, M., Fernandez-pello, C., Urban, D. L., Ruff, G. A. & Olson, S. L. On simulating concurrent flame spread in reduced gravity by reducing ambient pressure. *Proc. Combust. Inst.* **37**, 3793–3800 (2019).
23. Thomsen, M., Fernandez-Pello, C., Ruff, G. A. & Urban, D. L. Buoyancy effects on concurrent flame spread over thick PMMA. *Combust. Flame* **199**, 279–291 (2019).
24. Thomsen, M., Huang, X., Fernandez-Pello, C., Urban, D. L. & Ruff, G. A. Concurrent flame spread over externally heated Nomex under mixed convection flow. *Proc. Combust. Inst.* **37**, 3801–3808 (2019).
25. McAllister, S., Fernandez-Pello, C., Urban, D. & Ruff, G. The combined effect of pressure and oxygen concentration on piloted ignition of a solid combustible. *Combust. Flame* **157**, 1753–1759 (2010).
26. De Ris, J. N. Spread of a laminar diffusion flame. *Symp. Combust.* **12**, 241–252 (1969).
27. Fernandez-pello, A. C. Modelling flame spread as a flame induced solid ignition process. *Fire Explos. Hazards Proc. fourth Int. Semin.* 13–26 (2004).
28. Mao, C.-P., Fernandez-Pello, A. C. & Pagni, P. J. Mixed convective buring of a fuel surface with arbitrary inclination. *J Heat Transf.* **106**, 304–309 (1984).